J. Phys. B: At. Mol. Opt. Phys. **23** (1990) 3335-3351. Printed in the UK

The second Born approximation for electron loss to the continuum

D H Jakubaßa-Amundsen

Sektion Physik, Universität München, 8046 Garching, Federal Republic of Germany

Received 5 December 1989, in final form 4 May 1990

Abstract. The spectral distribution of projectile electrons which are ejected into the forward direction in fast ion-atom collisions is calculated in the second-order Born theory. A skewness of the forward peak is found which is, however, much weaker than in the case of electron capture to the continuum. The peak asymmetry, the width as well as total cusp cross sections are calculated for $He^+ + He$ collisions and compared with the available experimental data.

1. Introduction

During the recent years, great effort has been devoted to the investigation of electrons which are ejected with small momenta relative to the projectile (Groeneveld *et al* 1984). For partly stripped projectiles, these electrons originate from two different processes: Capture of target electrons to the projectile continuum (CTC) and loss of projectile electrons to the continuum (ELC), the latter process being dominant at high collision velocities v.

The basic difference in the theoretical description of the two processes becomes apparent in the limit of very high projectile velocities. While an exact CTC theory reduces asymptotically to the second-order Born approximation (Dettmann *et al* 1974, Shakeshaft and Spruch 1978, Jakubaßa-Amundsen 1989*a*), ELC is described within the first-order Born approximation (Drepper and Briggs 1976, Briggs and Drepper 1978, Day 1981, Burgdörfer *et al* 1983). These two approximations differ in the predictions for the shape of the forward peak which appears in the electron spectrum at electron momenta $\boldsymbol{k}_f$ close to $\boldsymbol{v}$. The first-order Born approximation provides a symmetric peak, while higher-order perturbative terms introduce an asymmetry, enhancing the electron intensity for $k_f < v$ as compared with $k_f > v$. For CTC, a strong peak skewness is manifest in many experimental data (Breinig *et al* 1982, Knudsen *et al* 1986a, Gulyás *et al* 1986). Experimental electron loss peaks, on the other hand, are nearly symmetric, and eventually occurring asymmetries have commonly been interpreted as resulting from a CTC contamination (Breinig *et al* 1981, Kövér *et al* 1986, Man *et al* 1986a). Recent compilations of ELC data from a variety of collision systems show, however, systematics in the peak asymmetry which require the inclusion of higher-order Born terms even in the case of electron loss (Lucas and Steckelmacher 1987, Atan *et al* 1990).

Theoretical investigations of the electron loss peak in the forward direction have mostly been carried out within the first Born approximation (Drepper and Briggs 1976), one exception being a higher-order approach which is based on the Faddeev equations

0953-4075/90/193335+17$03.50

(Jakubaßa-Amundsen 1981). The Born approximation has subsequently been modified to allow for a simultaneous excitation of the target electrons during the ELC process (Briggs and Drepper 1978, Burgdörfer *et al* 1983) which has been found to be very important at all impact velocities (Day 1981). Recently, the inclusion of target excitation has also been combined with the treatment of ELC within the peaked impulse approximation, particularly suited for heavy target atoms (Hartley and Walters 1987).

In the present work, the electron-target interaction is included to second order, both in the 'elastic' contribution (also termed singly inelastic cross section) where the target atom remains in its ground state, as well as in the 'inelastic' contribution (also termed doubly inelastic cross section) where the target goes over into an excited state. The theory is formulated in section 2, and numerical results for the spectral distribution of the ELC electrons, the peak asymmetry and shape parameters, and the integral peak cross sections are given in section 3. In order to display the respective magnitude and velocity dependence of the elastic and inelastic contributions to ELC, the shape parameters are calculated separately for the two processes. We have selected the symmetric collision system $He^+ + He$ as it provides an ideal test case for the second-order Born theory down to rather low collision velocities ($v \geq 2$), but also because it is extensively studied experimentally (Knudsen *et al* 1986b, Man *et al* 1986b, Gulyás *et al* 1986). The conclusions are drawn in section 4. Atomic units ($\hbar = m = e = 1$) are used unless otherwise indicated.

2. Theory

Restricting ourselves to a one-electron projectile and describing the internuclear motion by a classical trajectory, the collision is governed by the electronic Hamiltonian

$$H = H_P + H_T + V_{eT} + V_{ee} + V_{Pe} \tag{2.1}$$

where H_P and H_T refer to the isolated projectile and target, respectively, V_{eT} denotes the interaction of the projectile electron with the target nucleus, V_{ee} is the interaction of the projectile electron with all N target electrons, and V_{Pe} describes the interaction between the projectile nucleus and the target electrons

$$V_{eT} = -\frac{Z_T}{r_T} \qquad V_{ee} = \sum_{m=1}^{N} \frac{1}{|\boldsymbol{r}_T - \boldsymbol{r}_{mT}|} \qquad V_{Pe} = -Z_P \sum_{m=1}^{N} \frac{1}{|\boldsymbol{r}_{mT} - \boldsymbol{R}|}. \tag{2.2}$$

Z_P and Z_T are the nuclear charges of the projectile and target, respectively, and the coordinates are depicted in figure 1. The transition amplitude for exciting the projectile electron from its initial bound state ψ_i^P (with energy ε_i) to the final continuum state

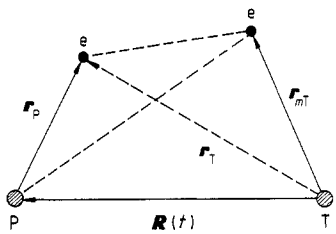

Figure 1. Coordinates for the collision system consisting of the projectile nucleus (P), the target nucleus (T) and the electrons (e). Only one target electron is shown.

ψ_f^P (with energy ε_f) and allowing simultaneously for target excitation, is in the second-order Born approximation given by the time integral

$$a_{fi} = -i \int dt \langle \phi_f^T \psi_f^P | V_{eT} + V_{ee} | \psi_i^P \phi_i^T \rangle - i \int dt \langle \phi_f^T \psi_f^P | (V_{eT} + V_{ee}) G_P (V_{eT} + V_{ee}) + V_{Pe} G_P (V_{eT} + V_{ee}) + (V_{eT} + V_{ee}) G_P V_{Pe} | \psi_i^P \phi_i^T \rangle \quad (2.3)$$

where ϕ_i^T (with energy E_i) and ϕ_f^T (with energy E_f) are eigenstates to H_T which describe the target electrons in their initial and final state, respectively, and $G_P = (i\partial_t - H_P - H_T + i\varepsilon)^{-1}$ is the propagator of the unperturbed system. The coupling V_{Pe} does not contribute to first order and nor does it couple $V_{Pe} G_P V_{Pe}$ to second order because of the orthogonality of the projectile states ψ_f^P and ψ_i^P.

2.1. Elastic contribution to ELC

The transition amplitude for the elastic contribution is obtained from (2.3) by replacing ϕ_f^T by the target ground state ϕ_i^T, which is approximated by a Slater determinant of single-particle Hartree–Fock states $\{\varphi_n^T(\boldsymbol{r}); n = 1, \ldots N\}$. In the first-order term of (2.3), the effective electron-target interaction is given by

$$V_T(\boldsymbol{r}_T) = V_{eT} + \langle \phi_i^T | V_{ee} | \phi_i^T \rangle \quad (2.4)$$

This Hartree–Fock potential can to sufficient accuracy be fitted by a sum of exponentials (Strand and Bonham 1964), the Fourier transform of which is given by

$$\tilde{V}_T(\boldsymbol{q}) = -\left(\frac{2}{\pi}\right)^{1/2} Z_T \left(\sum_{i=1}^{2} \frac{a_i}{q^2 + b_i^2} + \sum_{i=1}^{3} \frac{2\alpha_i \beta_i}{(q^2 + \beta_i^2)^2} \right) \quad (2.5)$$

where the coefficients a_i, b_i, α_i and β_i are the fit parameters. Note that $\tilde{V}_T$ can alternatively be expressed in terms of the elastic form factor F_{el} of the target, $\tilde{V}_T(q) = -(2/\pi)^{1/2}[Z_T - F_{el}(q)]/q^2$ (Rule 1977, Briggs and Taulbjerg 1978), where

$$F_{el}(q) = \sum_{n=1}^{N} \langle \varphi_n^T | e^{-i\boldsymbol{q}\boldsymbol{r}} | \varphi_n^T \rangle \quad (2.6)$$

has to be calculated numerically.

In order to simplify the evaluation of the second-order terms in the transition amplitude, we approximate $V_{eT} + V_{ee}$ throughout by the effective electron-target interaction $V_T(\boldsymbol{r}_T)$. As a consequence of neglecting electron correlations in the second-order term through the 'single-particle' approximation $V_{eT} + V_{ee} \approx V_T$, there are no couplings to intermediate excited target states $\phi_{n'}^T$. Hence, terms like $V_{Pe} G_P (V_{eT} + V_{ee})$ in (2.3) do not contribute to the target ground state—ground state scattering. The transition amplitude for the elastic contribution to electron loss reduces therefore to

$$a_{fi}^{el} \equiv a_{fi}^{(1,el)} + a_{fi}^{(2,el)} = -i \int dt \langle \psi_f^P | V_T | \psi_i^P \rangle - i \int dt \langle \phi_i^T \psi_f^P | V_T G_P V_T | \psi_i^P \phi_i^T \rangle \quad (2.7)$$

The first-order transition amplitude is readily evaluated with the help of the Fourier representation of V_T, if the internuclear coordinate is approximated by a straight-line path with impact parameter b, $\boldsymbol{R}(t) = \boldsymbol{b} + \boldsymbol{v}t$. One obtains

$$a_{fi}^{(1,el)} = -\frac{i}{(2\pi)^{1/2}} \int d\boldsymbol{q}\, \tilde{V}_T(\boldsymbol{q}) \delta(\varepsilon_f - \varepsilon_i + \boldsymbol{q}\boldsymbol{v}) \exp(i\boldsymbol{q}\cdot\boldsymbol{b}) \langle \psi_f^P(\boldsymbol{r}_P) | \exp(i\boldsymbol{q}\cdot\boldsymbol{r}_P) | \psi_i^P(\boldsymbol{r}_P) \rangle. \quad (2.8)$$

For the calculation of the second-order term in (2.7), the spectral representation of G_P is used

$$G_P V_T(t) = \frac{1}{2\pi} \int dt' \, d\omega \sum_{n,n'} |\psi_n^P \phi_{n'}^T\rangle \frac{\exp[-i\omega(t-t')]}{\omega - \varepsilon_n - E_{n'} + i\varepsilon} \langle \psi_n^P \phi_{n'}^T | V_T(t') \qquad (2.9)$$

where a complete set of eigenstates to $H_P + H_T$, $\psi_n^P * \phi_{n'}^T$ with energies $\varepsilon_n + E_{n'}$ has been introduced. When (2.9) is inserted into the second-order transition matrix element, the target states $\phi_{n'}^T$ drop out because they are not affected by the single-particle potential V_T. Introducing the Fourier transform of V_T, the integrals over t, t' and ω can immediately be carried out, and one finds

$$a_{fi}^{(2,el)} = -\frac{i}{4\pi^2} \sum_n \int ds \, dq \, \tilde{V}_T(s) \tilde{V}_T(q-s) \frac{1}{v \cdot s + \varepsilon_f - \varepsilon_n + i\varepsilon} \exp(iq \cdot b)$$

$$\times \delta(\varepsilon_f - \varepsilon_i + q \cdot v) \langle \psi_f^P | \exp(is \cdot r_P) | \psi_n^P \rangle \langle \psi_n^P | \exp[i(q-s) \cdot r_P] | \psi_i^P \rangle. \qquad (2.10)$$

For the further evaluation of $a_{fi}^{(2,el)}$ two additional approximations are made. Firstly, only K and L shells are explicitly considered in the sum over the intermediate states ψ_n^P, whereas the higher-lying states are accounted for by a closure approximation (Holt and Moiseiwitsch 1968). This approximation is reasonable for electron loss from the K shell (Gayet 1989). The average energy $\bar{\varepsilon}_n$ for the higher-lying states is set equal to the energy of the lowest of these states (the 3s state). This is, however, of no serious consequence since the dependence of the cross section on $\bar{\varepsilon}_n$ is rather weak. Secondly, we introduce a peaking approximation which affects only those terms in the sum over n which are explicitly considered. This so-called 'transverse' peaking approximation relies on the fact that $\tilde{V}_T(q-s)$ is strongly peaked at $q = s$ (cf equation (2.5)). Since the δ-function in (2.10) requires q to be predominantly in the z direction (along v), the main contribution arises from small transverse components $s_\perp$ (perpendicular to v). Also taking into consideration that $\tilde{V}_T(s)$ is peaked at $s_\perp = 0$, one can approximate the momentum s in the weakly varying matrix elements of (2.10) by $s_z e_z$ which allows for an analytic evaluation of the integral over $s_\perp$.

The doubly differential cross section for the emission of projectile electrons with energy E_f into the solid angle $d\Omega_f$ (in the target frame of reference), leaving the target in its ground state, is calculated from the sum of (2.8) and (2.10)

$$\frac{d^2\sigma^{el}}{dE_f \, d\Omega_f} = k_f \int db \, |a_{fi}^{(1,el)} + a_{fi}^{(2,el)}|^2$$

$$= \frac{4\pi k_f}{v^2} \int_{q_{min}}^{\infty} q \, dq \int_0^{\pi} d\varphi_q \Bigg| \tilde{V}_T(q) \langle \psi_f^P | \exp(iq \cdot r_P) | \psi_i^P \rangle$$

$$+ (2\pi)^{-3/2} \int_{-\infty}^{\infty} ds_z \left(\int ds_\perp \tilde{V}_T(s) \tilde{V}_T(q-s) \right)$$

$$\times \left(\sum_{n=1,2} \left(\frac{1}{vs_z + \varepsilon_f - \varepsilon_n + i\varepsilon} - \frac{1}{vs_z + \varepsilon_f - \bar{\varepsilon}_n + i\varepsilon} \right) \right.$$

$$\times \langle \psi_f^P | \exp(is_z e_z \cdot r_P) | \psi_n^P \rangle \langle \psi_n^P | \exp[i(q - s_z e_z) \cdot r_P] | \psi_i^P \rangle$$

$$\left. + \frac{1}{vs_z + \varepsilon_f - \bar{\varepsilon}_n + i\varepsilon} \langle \psi_f^P | \exp(iq \cdot r_P) | \psi_i^P \rangle \right) \Bigg|^2 \qquad (2.11)$$

where spherical coordinates have been chosen for $\boldsymbol{q}$. The minimum momentum transfer is given by $q_{\min} = (\varepsilon_f - \varepsilon_i)/v$, and the polar angle is obtained from $\cos\vartheta_q = -(\varepsilon_f - \varepsilon_i)/qv$. The three integrals over q, φ_q and s_z have to be done numerically. Explicit expressions for the matrix elements in (2.11) and for the integral over $s_\perp$ are given in the appendix.

2.2. *Inelastic contribution to* ELC

The transition amplitude for the inelastic process is obtained from (2.3) with $\phi_f^{\mathrm{T}} \neq \phi_i^{\mathrm{T}}$. Due to the orthogonality of these target states, only the electron–electron potential V_{ee} contributes to first order. When the single-particle approximation, $V_{\mathrm{eT}} + V_{\mathrm{ee}} \approx V_{\mathrm{T}}$ is used in the second-order term, there is also no contribution from the coupling $(V_{\mathrm{eT}} + V_{\mathrm{ee}}) G_{\mathrm{P}} (V_{\mathrm{eT}} + V_{\mathrm{ee}})$. This approximation is somewhat more severe than the corresponding one in the elastic case, because electron correlations are more important if also the target is excited, but also because inelastic ELC dominates over the elastic one. To neglect a term with $V_{\mathrm{ee}} G_{\mathrm{P}} V_{\mathrm{T}}$ as compared with $V_{\mathrm{Pe}} G_{\mathrm{P}} V_{\mathrm{T}}$ is only justified for heavy projectiles where the projectile interaction V_{Pe} is considerably stronger than the electron–electron coupling. This condition is not very well satisfied for He^+ projectiles, but the single-particle approximation will give reasonable results as long as the second Born term is smaller than the first Born term, i.e. in the validity regime of the second-order Born approximation. Hence, the transition amplitude for the inelastic ELC contribution reads

$$\begin{aligned} a_{fi}^{\mathrm{in}} &\equiv a_{fi}^{(1,\mathrm{in})} + a_{fi}^{(2,\mathrm{in})} \\ &= -\mathrm{i} \int \mathrm{d}t \langle \phi_f^{\mathrm{T}} \psi_f^{\mathrm{P}} | V_{\mathrm{ee}} | \psi_i^{\mathrm{P}} \phi_i^{\mathrm{T}} \rangle \\ &\quad -\mathrm{i} \int \mathrm{d}t \langle \phi_f^{\mathrm{T}} \psi_f^{\mathrm{P}} | V_{\mathrm{Pe}} G_{\mathrm{P}} V_{\mathrm{T}} + V_{\mathrm{T}} G_{\mathrm{P}} V_{\mathrm{Pe}} | \psi_i^{\mathrm{P}} \phi_i^{\mathrm{T}} \rangle. \end{aligned} \tag{2.12}$$

With the Fourier representation of the electron–electron interaction, the first-order term is given by

$$\begin{aligned} a_{fi}^{(1,\mathrm{in})} = -\frac{\mathrm{i}}{\pi} \int \frac{\mathrm{d}\boldsymbol{q}}{q^2} \delta(E_f - E_i + \varepsilon_f - \varepsilon_i + \boldsymbol{q}\cdot\boldsymbol{v}) \exp(\mathrm{i}\boldsymbol{q}\cdot\boldsymbol{b}) \\ \times \langle \phi_f^{\mathrm{T}} | \sum_m \exp(-\mathrm{i}\boldsymbol{q}\cdot\boldsymbol{r}_{m\mathrm{T}}) | \phi_i^{\mathrm{T}} \rangle \langle \psi_f^{\mathrm{P}} | \exp(\mathrm{i}\boldsymbol{q}\cdot\boldsymbol{r}_{\mathrm{P}}) | \psi_i^{\mathrm{P}} \rangle. \end{aligned} \tag{2.13}$$

The evaluation of the second-order term proceeds in an analogous way as for the elastic case. Inserting a complete set of eigenstates $\psi_n^{\mathrm{P}} * \phi_{n'}^{\mathrm{T}}$ and noting that due to the single-particle nature of V_{T} and V_{Pe}, couplings to intermediate states with $n, n' \neq \{i, f\}$ do not occur, one obtains

$$\begin{aligned} a_{fi}^{(2,\mathrm{in})} = -\frac{\mathrm{i}}{2\pi} \int \mathrm{d}t\, \mathrm{d}t'\, \mathrm{d}\omega \exp[\mathrm{i}(E_f + \varepsilon_f)t] \Big(\langle \phi_f^{\mathrm{T}} | V_{\mathrm{Pe}}(t) | \phi_i^{\mathrm{T}} \rangle \frac{\exp[-\mathrm{i}\omega(t-t')]}{\omega - \varepsilon_f - E_i + \mathrm{i}\varepsilon} \\ \times \langle \psi_f^{\mathrm{P}} | V_{\mathrm{T}}(\boldsymbol{r}_{\mathrm{P}} + \boldsymbol{R}(t')) | \psi_i^{\mathrm{P}} \rangle + \langle \psi_f^{\mathrm{P}} | V_{\mathrm{T}}(\boldsymbol{r}_{\mathrm{P}} + \boldsymbol{R}(t)) | \psi_i^{\mathrm{P}} \rangle \\ \times \frac{\exp[-\mathrm{i}\omega(t-t')]}{\omega - \varepsilon_i - E_f + \mathrm{i}\varepsilon} \langle \phi_f^{\mathrm{T}} | V_{\mathrm{Pe}}(t') | \phi_i^{\mathrm{T}} \rangle \Big) \exp[-\mathrm{i}(E_i + \varepsilon_i)t']. \end{aligned} \tag{2.14}$$

When the Fourier representations of V_{Pe} and V_T are inserted, the time and frequency integrals can be carried out and the transition amplitude reduces to

$$a_{fi}^{(2,in)} = \frac{Z_P}{\sqrt{2}\,\pi^{3/2}} \int d\boldsymbol{q}\, \delta(E_f - E_i + \varepsilon_f - \varepsilon_i + \boldsymbol{q}\cdot\boldsymbol{v}) \exp(i\boldsymbol{q}\cdot\boldsymbol{b}) \int \frac{d\boldsymbol{s}}{s^2}\, \tilde{V}_T(\boldsymbol{q}+\boldsymbol{s})\delta(E_f - E_i - \boldsymbol{s}\cdot\boldsymbol{v})$$
$$\times \left\langle \phi_f^T \middle| \sum_{m=1}^{N} \exp(i\boldsymbol{s}\cdot\boldsymbol{r}_{mT}) \middle| \phi_i^T \right\rangle \langle \psi_f^P | \exp[i(\boldsymbol{q}+\boldsymbol{s})\cdot\boldsymbol{r}_P] | \psi_i^P \rangle \tag{2.15}$$

where use has been made of the relation $(a+i\varepsilon)^{-1} - (a-i\varepsilon)^{-1} = -2\pi i\,\delta(a)$.

For the further evaluation the transverse peaking approximation is applied to set $s_\perp = 0$ in the two matrix elements of (2.15). Since $s_z = (E_f - E_i)/v$ is fixed by the δ-function, the $\boldsymbol{s}$-integral reduces to a convolution of the potentials. From (2.13) and (2.15), the doubly differential cross section for electron loss with simultaneous target excitation is thus given by

$$\frac{d^2\sigma^{in}}{dE_f\, d\Omega_f} = \frac{4k_f}{v} \sum\!\!\!\!\!\!\int_{f>N} \sum_{n=1}^{N} \int d\boldsymbol{q}\, \delta(E_f^T - E_n^T + \varepsilon_f - \varepsilon_i + \boldsymbol{q}\boldsymbol{v})$$
$$\times |\langle \varphi_f^T | A \exp(-i\boldsymbol{q}\cdot\boldsymbol{r}) + B \exp(is_z\boldsymbol{e}_z\cdot\boldsymbol{r}) | \varphi_n^T \rangle|^2$$
$$A = -\frac{i}{q^2} \langle \psi_f^P | \exp(i\boldsymbol{q}\cdot\boldsymbol{r}_P) | \psi_i^P \rangle \tag{2.16}$$
$$B = \frac{Z_P}{\sqrt{2\pi}v} \left(\int \frac{d\boldsymbol{s}_\perp}{s^2}\, \tilde{V}_T(\boldsymbol{q}+\boldsymbol{s}) \right) \langle \psi_f^P | \exp[i(\boldsymbol{q} + s_z\boldsymbol{e}_z)\cdot\boldsymbol{r}_P] | \psi_i^P \rangle$$

where φ_n^T denotes the bound states of the ground-state configuration ϕ_i^T, while φ_f^T is a state above the Fermi level (indicated by the symbol $f > N$), and $E_f^T - E_n^T$ is the energy difference of the states φ_f^T and φ_n^T. As first- and second-order terms in (2.16) have the same structure, the sum over the final target states is readily evaluated if the excitation energy is approximated by a fixed value, $E_f^T - E_n^T \simeq \Delta\bar{E}_{fi}$, such that closure can be applied. Following Day (1981), we choose $\Delta\bar{E}_{fi} = |\varepsilon_{1s}^T| + \kappa_f^2/2$ where ε_{1s}^T is the target K-shell energy and $\boldsymbol{\kappa}_f = \boldsymbol{k}_f - \boldsymbol{v}$ the momentum of the ejected electron in the projectile reference frame. Since $\sum\!\!\!\!\!\!\int_{f>N} = \sum\!\!\!\!\!\!\int_f - \Sigma_{k=1}^N$, the inelastic contribution to ELC reduces to

$$\frac{d^2\sigma^{in}}{dE_f\, d\Omega_f} = \frac{8k_f}{v^2} \int_{\bar{q}_{min}}^{\infty} q\, dq \int_0^{\pi} d\varphi_q \Big(|A|^2 S_{in}(q) + |B|^2 S_{in}(s_z) + 2\,\mathrm{Re}\{A^* B F_{el}(|\boldsymbol{q} + s_z\boldsymbol{e}_z|)\}$$
$$- \sum_{n,k=1}^{N} 2\,\mathrm{Re}\{A^* B \langle \varphi_n^T | \exp(i\boldsymbol{q}\cdot\boldsymbol{r}) | \varphi_k^T \rangle \langle \varphi_k^T | \exp(is_z\boldsymbol{e}_z\cdot\boldsymbol{r}) | \varphi_n^T \rangle\} \Big) \tag{2.17}$$
$$S_{in}(p) = N - \sum_{n,k=1}^{N} |\langle \varphi_k^T | \exp(i\boldsymbol{p}\cdot\boldsymbol{r}) | \varphi_n^T \rangle|^2$$

where $\bar{q}_{min} = (\Delta\bar{E}_{fi} + \varepsilon_f - \varepsilon_i)/v$, $\cos\vartheta_q = -\bar{q}_{min}/q$ and $s_z = \Delta\bar{E}_{fi}/v$. $\mathrm{Re}\{M\}$ denotes the real part of M, $F_{el}(p)$ is the elastic form factor, equation (2.6), and $S_{in}(p)$ is the incoherent scattering form factor (Kim and Inokuti 1968, Rule 1977). Explicit expressions for the matrix elements as well as for the integral over $s_\perp$ occurring in A and B are given in the appendix. The transition matrix elements of the target in the last term of (2.17) have to be calculated numerically with, e.g., the help of the Roothaan-Hartree-Fock wavefunctions as tabulated by Clementi and Roetti (1974).

For the special case of a He target the set $\{\varphi_n^T\}$ consists of only one spatial wavefunction (with two spin degrees of freedom). Therefore, the inelastic cross section is completely determined by F_{el}, since for He, one has in addition $S_{in} = 2 - F_{el}^2/2$ (Briggs and Taulbjerg 1978)

$$\frac{d^2\sigma^{in}}{dE_f\, d\Omega_f}(\mathrm{He}) = \frac{8k_f}{v^2}\int_{\bar{q}_{min}}^{\infty} q\, dq \int_0^{\pi} d\varphi_q [2|A|^2 + 2|B|^2 - \tfrac{1}{2}|AF_{el}(q)|^2 - \tfrac{1}{2}|BF_{el}(s_z)|^2 + 2\,\mathrm{Re}\{A^*B\}(F_{el}(|\boldsymbol{q} + s_z\boldsymbol{e}_z|) - \tfrac{1}{2}F_{el}(q)F_{el}(s_z))]. \tag{2.18}$$

The total doubly differential cross section for electron loss is determined by the sum of the elastic and inelastic contributions, (2.11) + (2.18).

3. The peak shape in comparison with experiment

The structure of the electron distribution in the vicinity of the projectile threshold is readily extracted from the limit $\kappa_f \to 0$ of the ionization matrix element which appears in the integrands of both the elastic and inelastic ELC contribution. For a 1s initial state one obtains from formula (A.2) of the appendix

$$\langle \psi_f^P | \exp(i\boldsymbol{q}\cdot\boldsymbol{r}) | \psi_{1s}^P \rangle \to \frac{8Z_P^3}{(\pi\kappa_f)^{1/2}} \exp[i \arg \Gamma(1 - i\eta_f)] \frac{\exp[-2Z_P^2/(Z_P^2 + q^2)]}{(Z_P^2 + q^2)^2} \times \exp\left(-2iZ_P q \frac{\cos\vartheta}{Z_P^2 + q^2}\right) \qquad \kappa_f \to 0 \tag{3.1}$$

where $\eta_f = Z_P/\kappa_f$ and $\cos\vartheta = \cos\theta_f' \cos\vartheta_q + \sin\theta_f' \sin\vartheta_q \cos\varphi_q$ with θ_f' the electron emission angle in the projectile reference frame. Similar expressions hold for the higher bound projectile states ψ_n^P. Two features are obvious from (3.1). First, the cross section shows the well known divergence with κ_f^{-1} (Drepper and Briggs 1976). The finite peak height in the experimental spectra is just a consequence of the finite detector resolution, and in order to compare with experiment, the theoretical cross section has to be averaged over the angular resolution θ_0 (assuming that the energy resolution is good enough, so that its influence can be neglected)

$$\left\langle \frac{d^2\sigma}{dE_f\, d\Omega_f} \right\rangle = \frac{1}{1 - \cos\theta_0} \int_0^{\theta_0} \sin\vartheta_f\, d\vartheta_f \left(\frac{d^2\sigma^{el}}{dE_f\, d\Omega_f} + \frac{d^2\sigma^{in}}{dE_f\, d\Omega_f} \right) \tag{3.2}$$

where ϑ_f is the electron emission angle in the target frame of reference.

The second feature in the electron spectrum concerns the peak asymmetry. From (3.1) it follows that even in the limit $\kappa_f \to 0$, there remains a dependence on the emission angle θ_f' which allows for different emission intensities on the left-hand side of the peak ($k_f \lesssim v$, $\theta_f' = 180°$) and on the right-hand side ($k_f \gtrsim v$, $\theta_f' = 0°$). As this θ_f' dependence occurs only in a phase factor, it disappears upon squaring and hence is not present in the first-order Born approximation such that the peak is symmetric (Day 1980). If, however, higher-order Born terms are included, there remains a net dependence on θ_f' because the different phases of the Born terms can interfere, but also because the higher Born terms have a θ_f'-dependent modulus. The approximations for these terms must, however, be chosen carefully in order to retain this θ_f' dependence (note e.g. that if the usual closure approximation were used in the elastic ELC contribution without explicit consideration of the $n = 1, 2$ projectile states in (2.11), there were no θ_f' dependence left).

In contrast to electron capture to the continuum (Jakubaßa-Amundsen 1988, 1989b), the prefactor of $\cos\vartheta$ in the last phase factor of (3.1) is *finite* for any momentum q which means that the cross section is *analytic* in θ_f'. This remains true if one goes beyond the second Born approximation as has been done in the Faddeev-based approach (Jakubaßa-Amundsen 1981). Hence, it is reasonable to transform the cross section into the projectile frame of reference and expand it in terms of Legendre polynomials $P_l(\cos\theta_f')$, a method which has frequently been applied by the experimentalists in order to extract generic ELC cross sections which should be independent of the detector resolution (Meckbach *et al* 1981)

$$\frac{d^2\sigma}{dE_f\,d\Omega_f}=\frac{k_f}{\kappa_f}\frac{d^2\sigma}{d\varepsilon_f\,d\Omega_f'}=\frac{k_f}{\kappa_f}\sum_{n,l=0}^{\infty}B_{nl}\kappa_f^n P_l(\cos\theta_f') \tag{3.3}$$

Near the peak maximum at $\kappa_f=0$, only the expansion coefficients B_{0l} are important. Theoretically, they are obtained from the formula

$$B_{0l}=\frac{2l+1}{2}\int_{-1}^{1}d(\cos\theta_l')P_l(\cos\theta_f')\left[\frac{\kappa_f}{k_f}\frac{d^2\sigma}{dE_f\,d\Omega_f}\right]_{\kappa_f=0} \tag{3.4}$$

The first coefficients have a simple interpretation: B_{00} determines the magnitude of the cross section in the peak, B_{01} the peak skewness, i.e. the difference for $\theta_f'=0°$ and 180°, and B_{02} the anisotropy, i.e. the difference between transverse emission ($\theta_f'=90°$) and longitudinal emission. Commonly, only these three coefficients (together with those for $n=1$) are retained in a fit to the experimental spectrum. It should be noted that the next ones, B_{0l} with $l\geqslant 3$, are again absent in the first-order Born approximation for K-shell electron loss (Day 1980, Burgdörfer *et al* 1983), hence their presence is an indication of higher-order Born contributions, however hardly accessible experimentally within the present accuracy of the data.

We have calculated the cross section and the coefficients B_{0l}, $l\leqslant 2$ for the collision system $He^+ + He$ as a function of the collision velocity. For the He target, we have used the Hartree-Fock form factor $F_{el}(q)$ as tabulated in Kim and Inokuti (1968; together with a fitted tail $\sim q^{-3.5}$ for $q>10$). For the effective target potential V_T we have only used a two-term formula instead of (2.5) with the coefficients a_1, b_1, α_1, β_1 from Strand and Bonham (1964), but with $\alpha_2=0$ (since $\beta_2\gg\beta_1$, this underestimates the cross section by about 2%), while a_2 and α_3 vanish for He. The target binding energy is taken as $|\varepsilon_{1s}^T|=0.90359$. The numerical evaluation of the cross section is straightforward, and the singularities from the propagator are easily dealt with (see appendix).

The spectrum of electrons emitted in 2.6 MeV $He^+ + He$ collisions, integrated over the solid angle covered by the detector

$$\frac{d\sigma}{dk_f}(\theta_0)=2\pi k_f\int_0^{\theta_0}\sin\vartheta_f\,d\vartheta_f\frac{d^2\sigma}{dE_f\,d\Omega_f} \tag{3.5}$$

is depicted in figure 2. The detector resolution of the experimental set-up is 1.28° (Man *et al* 1986a); however, the use of a six-term expansion (3.3) with allowance for small variations in v and θ_0 in a least-squares fitting procedure to the experimental data, has led to an optimized value of $\theta_0=1.03°$ for this particular system (Atan *et al* 1990). We have performed second-order Born calculations for both values of θ_0: Although the experimental width of the peak is well reproduced when $\theta_0=1.03°$ is used, we find a much better agreement in the absolute cross section with the original value of θ_0.

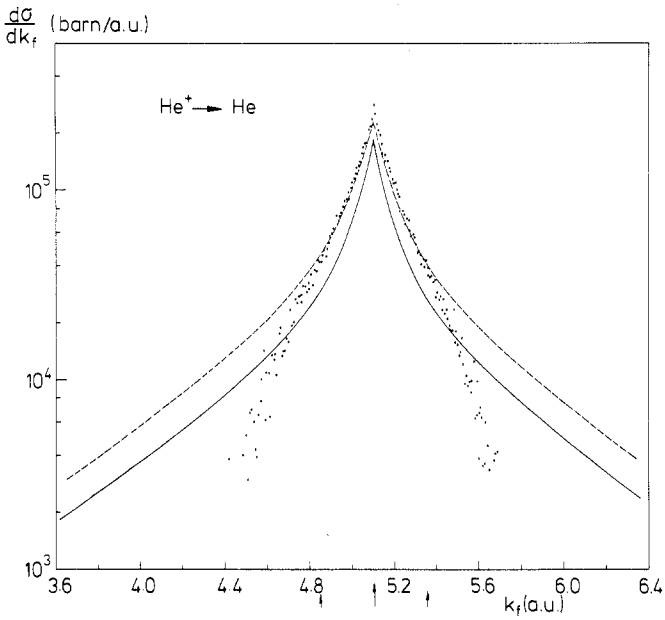

Figure 2. Angular integrated differential ELC cross section for 2.6 MeV $He^+ + He$ collisions. Shown are second Born calculations for a detector resolution of $\theta_0 = 1.28°$ (– – –) and 1.03° (——). The data points are from Lucas as described in Man *et al* (1986a). The large arrow denotes the peak position at $k_f = 5.1$, the small arrows are the limits of the truncated integration region (see text).

In figure 3, the results for B_{00} obtained from four different prescriptions are shown, inserting for $d^2\sigma/dE_f\, d\Omega_f$ in (3.4): (i) the total first-order Born result, (ii) the total second-order Born result, (iii) the elastic contribution $d^2\sigma^{el}/dE_f\, d\Omega_f$ from (2.11) and (iv) the inelastic contribution $d^2\sigma^{in}/dE_f\, d\Omega_f$ from (2.18). It is seen that at the lowest velocity considered, $v \simeq Z_P = 2$, the B_{00} calculated from the second-order theory (ii) is a factor of three above the first-order Born result, indicating the necessity of including still higher Born terms. On the other hand, for $v > 2Z_P$, the second-order Born term gives only a small correction to the first-order absolute cross sections. In any case, the dominant contribution to B_{00} arises from ionizing collisions which leave the target in an excited state. This is due to the fact that ELC from a charged projectile occurs at the same impact parameters which are relevant for exciting a target electron and transferring to it the same amount of momentum. The inelastic contribution is particularly important for small momentum transfer, while it is not that large for high momentum transfer (small v or large κ_f) since $\bar{q}_{min} > q_{min}$ (Briggs and Taulbjerg 1978).

Comparison is made with experimental data from three groups (Jensen 1986, Berényi and Gulyás 1989, Atan *et al* 1990). There is no obvious reason why the data fall below the total second-order Born result at high impact velocities. At low v, on the other hand, the strong increase of the data for decreasing v is due to the contamination with CTC electrons which have not been separated from the ELC electrons in the data of Berényi and Gulyás (1989) and Atan *et al* (1990). With the help of the impulse approximation (IA) for CTC (Jakubaßa-Amundsen 1988), we have estimated an upper and lower limit of the CTC contribution by means of the following consideration: the lower limit is obtained by calculating B_{00} for $H^+ + He$ collisions in the prior IA, valid

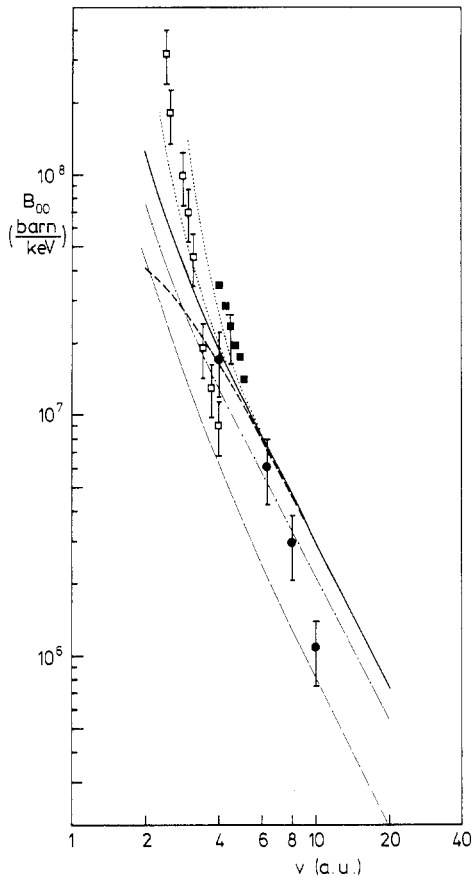

Figure 3. Peak height parameter B_{00} for $He^+ + He$ collisions as a function of the impact velocity v. The calculations include the second Born theory (——), the first Born theory (– – –), the elastic contribution (— —) as well as the inelastic contribution (–·–·–) to the second Born theory for ELC. The dotted curves result from an inclusion of the upper and lower limit, respectively, of the CTC contribution to B_{00}. The experimental data are from Berényi and Gulyás (1989) (▽), Atan *et al* (1990) (■) and Jensen (1986) as quoted e.g. in Lucas and Steckelmacher (1987) (●).

for $Z_P < Z_T$ (assuming that He^+ does not loose its electron during CTC), and adding about 30% of this value in order to account for the enhancement by the polarization of the bound electron of He^+ (Jakubaßa-Amundsen 1989b). The upper limit is obtained by calculating B_{00} for $He^{2+} + He$ in the post IA. This estimate for the order of magnitude of the CTC contribution agrees with the estimate by Jensen (1986) obtained from coincidence experiments. Adding these values for B_{00} to the ones for ELC leads to a reasonable agreement with the experimental data. At high velocities, CTC is completely negligible due to its rapid decrease with v.

In figure 4, the velocity dependence of the asymmetry parameters $\beta_1 = B_{01}/B_{00}$ and $\beta_2 = B_{02}/B_{00}$ is shown in comparison with the experimental data of Gulyás *et al* (1986), Atan *et al* (1990) and Knudsen *et al* (1986b). While $\beta_1 = 0$ in the first-order theory, the second-order Born approximation gives a negative β_1 in the whole velocity region investigated, indicating that like for CTC, the low-energy electrons ($k_f \lesssim v$) are emitted with a higher intensity than the electrons on the high-energy side of the peak ($k_f \gtrsim v$).

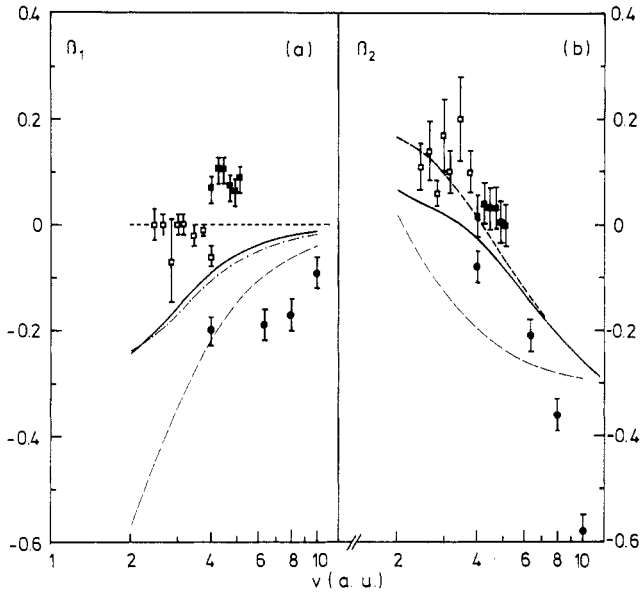

Figure 4. Skewness parameter $\beta_1(a)$ and anisotropy parameter β_2 (b) for $He^+ + He$ collisions as a function of the impact velocity v. The calculations include the second Born theory (——), the first Born theory (– – –) and the elastic contribution (— —) to the second Born theory for ELC. Shown also is the result for β_1 from a two-term expansion (– · – · –). The experimental data are taken from Gulyás *et al* (1986) and Berényi and Gulyás (1989) (□), as well as from Atan *et al* (1990) (■) and Knudsen *et al* (1986b) (●).

The velocity dependence of β_1 may be understood from an estimate of the θ_f'-dependent phase factor in the ionization matrix element (3.1). Inserting for $\boldsymbol{q}$ the most probable value $\boldsymbol{q} = \bar{q}_{\min}\boldsymbol{e}_z$ and assuming $Z_P \gtrsim Z_T$, one obtains the two limiting values

$$2Z_P q \frac{\cos\vartheta}{Z_P^2+q^2} \simeq -\cos\theta_f' \begin{cases} Z_P/v(1+2|\varepsilon_{1s}^T|/Z_P^2) & v \gg Z_P \\ 4v/Z_P(1+2|\varepsilon_{1s}^T|/Z_P^2)^{-1} & v \ll Z_P \end{cases} \tag{3.6}$$

At high velocities, the magnitude of this phase and thus $|\beta_1|$ increases proportional to Z_P/v and tends to zero for $v \to \infty$. This behaviour is also obtained in the impulse approximation for electron capture, but with a considerably higher prefactor of Z_P/v (Jakubaßa-Amundsen 1988). For electron loss, the scaling of β_1 with Z_P/v has been previously suggested from a simple binary-collision model and verified experimentally (Knudsen *et al* 1986b). At low collision velocities, (3.6) indicates that $|\beta_1|$ will have a maximum and then decrease again towards smaller v. A corresponding change in the slope of β_1 is evident in figure 4(a), but it should be kept in mind that at $v < Z_P$, higher-order Born terms have to be considered in the calculation.

In order to demonstrate the dependence of β_2 on the number of terms included in the series expansion (3.3), we have added in figure 4(a) the skewness parameter as calculated from a two-term expansion (considering only B_{00} and B_{01} which are obtained from the differential cross sections at $\theta_f' = 0°$ and 180° (Jakubaßa-Amundsen 1988)). The general velocity dependence is rather well approximated by this simple formula, but the magnitude of β_1 is somewhat overestimated.

The anisotropy parameter β_2 as shown in figure 4(b) is positive for small values of v and negative for large v, tending to a constant value at $v \to \infty$. This trend is similar

to that in the first Born approximation which has previously been used to calculate β_2 for $He^+ + H$ collisions (Burgdörfer *et al* 1983).

Figure 4 reveals also the importance of allowing for target excitation during ELC. Consideration of the elastic contribution alone would lead to a drastic overestimate of both $|\beta_1|$ and $|\beta_2|$ and would also result in an incorrect velocity dependence.

The fact that the experimental data from the different groups scatter far outside the error bars may point to a residual θ_0 dependence of the parameters B_{nl} from the truncated expansion (3.3), since the data analysing procedure has been cross-checked by the different groups with identical data (Atan *et al* 1990). Hence the ELC peak shape may alternatively be characterized by the full width at half maximum, Γ_{FWHM} which can easily be scaled with θ_0. Using a truncated series (3.3) with $n = 0$ and $l = 0, 2$ and integrating over the detector resolution, Day (1980) has found the following relation

$$\Gamma_{FWHM} = \tfrac{3}{2}\theta_0 v(1 + \tfrac{3}{2}\beta_2) \tag{3.7}$$

which should be more general than the first-order Born approximation upon which it is based. In fact, the scaling of Γ_{FWHM} with θ_0 has been applied successfully to a variety of data (Lucas and Steckelmacher 1987), and it is also realized in the second-order Born approximation to a very good extent (the change of Γ_{FWHM}/θ_0 is less than 3% when θ_0 is increased from 1° to 1.5°). In figure 5 we have plotted the velocity dependence

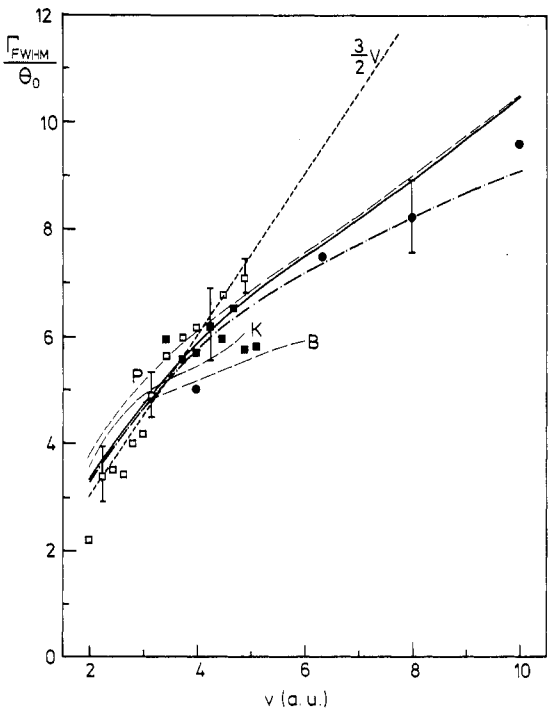

Figure 5. Scaled full width at half maximum, Γ_{FWHM}/θ_0, for ELC from $He^+ + He$ collisions as a function of the impact velocity v. Shown are results from the second Born approximation (——, $\theta_0 = 1.5°$), from Day's formula (3.8) (– · – · –, $\theta_0 = 1.5°$), the $\frac{3}{2}v$ line (– – –) as well as the first Born results (— —) from Burgdörfer (1986) (B, $\theta_0 = 1.28°$), from Kövér *et al* (1986) (K, $\theta_0 = 1.5°$) and the present result (P, $\theta_0 = 1.5°$). The experimental data from Kövér *et al* (□, $\theta_0 = 1.5°$), Man *et al* (■, $\theta_0 = 1.28°$) and Jensen (●, $\theta_0 = 1.61°$) are taken from the compilation by Lucas and Steckelmacher (1987).

of Γ_{FWHM}/θ_0 as calculated from the second-order Born theory, and it is seen that the prescription (3.7) (with β_2 from the second-order Born theory) provides a very good approximation up to $v \approx 5$. At the higher velocities, B_{nl} with $n > 0$ come into play because of the increasing peak width (Day 1980) and the second Born result shows a stronger increase with v than would be predicted by (3.7). It should be noted that the simple formula $\frac{3}{2}v\theta_0$ for Γ_{FWHM} which derives from considering the peak shape as being exclusively determined by the prefactor κ_f^{-1} in (3.3) (Dettmann *et al* 1974, Day 1980), fails already for $v \geqslant 4$.

For the sake of completeness, previous first-order Born results from Burgdörfer (1986) and Kövér *et al* (1986) have been included. Theory is compared with the experimental data from Jensen (1986), Kövér *et al* (1986) and Man *et al* (1986a) as compiled in Lucas and Steckelmacher (1987). It is found that the velocity dependence of the data can be fairly well reproduced by the second-order Born theory, whereas the first Born approximation is incorrect at the lower velocities.

Total cusp cross sections are obtained upon integrating over the spectral distribution. Figure 6 shows the velocity dependence of the cusp cross sections from a first-order and a second-order Born calculation with an integration interval covering the whole ELC peak region. In contrast to the fact that B_{00} strongly decreases with increasing velocity, the total cusp cross section decreases only weakly for $v \geqslant 4$ because both the peak width and the available phase space in the target frame increase with v (Briggs and Drepper 1978). The second-order Born term becomes important for $v \leqslant 4$ in consistency with the result for B_{00} (figure 3), and leads to a strong increase of the cusp cross section with decreasing v. This increase has also been found experimentally (Kövér *et al* 1986).

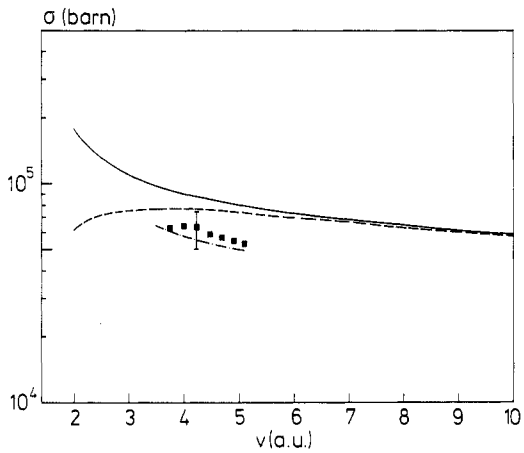

Figure 6. Total ELC cusp cross section for $He^+ + He$ collisions as a function of the collision velocity v at $\theta_0 = 1.28°$. Shown are the results from the second Born theory (——), the first Born theory (– – –) and the second Born theory with a truncated integration interval (–·–·–, see text). The experimental data (▪) are from Man *et al* (1986b).

The comparison between theoretical cusp cross sections and experimental data is complicated by several facts. One problem concerns the subtraction of the background which results mainly from target electrons, but also from ionization of the residual gas. As evident from figure 2, the subtraction of a linear background (Man *et al* 1986a) seriously underestimates the ELC cross section on the outer wings of the peak. Another

problem concerns the strong dependence of the cusp cross section on the detector resolution, and there is no apparent simple scaling with θ_0. Finally, the cusp cross section depends on the integration interval which is truncated in different ways for the various data sets. In figure 6, we have therefore only included the data from Man *et al* (1986b) which all result from the choice of constant integration limits $k_f = v \pm 0.25$ (where the data still have a similar slope to theory, cf figure 2). If the same limits are taken in the second-order Born calculation, the data are nicely reproduced by theory, provided the resolution $\theta_0 = 1.28°$ is used, rather than the individually optimized values which scatter around 1.0°. Note, however, that this truncated integration interval yields only about 60% of the total cusp cross section.

4. Conclusion

We have applied the second-order Born theory to the study of the ELC process at forward emission angles. Singly as well as doubly inelastic ELC cross sections have been calculated up to second order with the help of the transverse peaking approximation as well as the conventional closure relation for the evaluation of the sum over the unobserved final states of the target electrons, and a less restrictive closure approximation for the consideration of intermediate excited projectile states. For the symmetric system investigated, $He^+ + He$ at a variety of impact velocities, we have found that for the total cross sections, the first Born approximation breaks down at velocities below twice the ground-state electronic orbiting velocity, and the second Born approximation becomes unreliable around $v \simeq Z_P$. As far as the peak shape is concerned, the skewness parameter $\beta_1 = B_{00}/B_{01}$ deviates considerably from the first Born result $\beta_1 = 0$. Its negative value indicates that the forward peak is skewed towards the low-energy side, however much weaker than in the case of electron capture to the continuum. This result is at variance with our previously obtained β_1 from the Faddeev-type approximation (Groeneveld *et al* 1984, p 17) but this may be due to the use of unscreened target wavefunctions in that approach.

The comparison with experimental data is complicated by the fact that the shape parameters B_{00}, β_1 and β_2 as measured by the different groups show strong variations. Hence, only an average experimental trend for these parameters can be extracted, and it is found that the second-order Born theory follows roughly this trend, although there are considerable deviations at the highest collision velocities considered. For the peak width Γ_{FWHM}, there exists a scaling with the detector resolution θ_0, and if Γ_{FWHM}/θ_0 is plotted over v, the data nearly merge within the error bars, and are quite well reproduced by the second Born approximation. As concerns the total, peak-integrated ELC cross sections, a comparison with the available experimental data is very intricate because the results depend not only on θ_0, but also on the momentum interval covered by the integration as well as on the particular method of background subtraction. We have found that the second Born theory can well describe the velocity dependence of the total cusp cross sections if the momentum interval around the peak maximum is truncated equally strongly in theory and experiment.

The present formalism is readily extended to multielectron projectiles and heavier targets where experimental data are also available (Jensen 1986, Man *et al* 1986a, b, Oswald *et al* 1989). In particular, we predict from (3.5) some increase of $|\beta_1|$ with target charge for the higher velocities; however, a thorough investigation will require much more numerical work than in the case of helium.

Acknowledgments

It is a pleasure to thank M W Lucas for many fruitful discussions, and J S Briggs, P A Amundsen and R Gayet for helpful comments. I should also like to thank H-D Betz for stimulating this project, and H Knudsen, M W Lucas, D Berényi and L Gulyás for the communication of unpublished data. Financial support from the GSI Darmstadt is gratefully acknowledged.

Appendix 1. Evaluation of the matrix elements for bound–bound and bound–continuum transitions of hydrogen-like projectiles as occur in equations (2.11) and (2.16)

For an initial 1s state and a final bound state in the K or L shell, one has ($\boldsymbol{r}_P \equiv \boldsymbol{r}$)

$$\begin{aligned}
&\langle\psi^P_{1s}|\exp(i\boldsymbol{p}\cdot\boldsymbol{r})|\psi^P_{1s}\rangle = 16Z_P^4/(p^2+4Z_P^2)^2\\
&\langle\psi^P_{2s}|\exp(i\boldsymbol{p}\cdot\boldsymbol{r})|\psi^P_{1s}\rangle = 4\sqrt{2}Z_P^4p^2/(p^2+\tfrac{9}{4}Z_P^2)^3\\
&\langle\psi^P_{2p,m}|\exp(i\boldsymbol{p}\cdot\boldsymbol{r})|\psi^P_{1s}\rangle = i4\sqrt{6\pi}[Z_P^5p/(p^2+\tfrac{9}{4}Z_P^2)^3]Y^*_{1m}(\hat{\boldsymbol{p}}).
\end{aligned} \tag{A.1}$$

The K-shell ionization matrix element is taken from McDowell and Coleman (1970):

$$\begin{aligned}
&\langle\psi^P_f|\exp(i\boldsymbol{q}\cdot\boldsymbol{r})|\psi^P_{1s}\rangle = N_0\frac{A_1^{-i\eta_f}(q)}{B_1^{2-i\eta_f}(\boldsymbol{q})}\left((1+i\eta_f)\frac{B_1(\boldsymbol{q})}{A_1(q)}+1-i\eta_f\right)\\
&A_n(q) = q^2-(\kappa_f+iZ_P/n)^2 \qquad B_n(\boldsymbol{q}) = Z_P^2/n^2+(\boldsymbol{\kappa}_f-\boldsymbol{q})^2\\
&N_0 = (2^{3/2}/\pi)Z_P^{5/2}\exp(\pi\eta_f/2)\Gamma(1-i\eta_f) \qquad \eta_f = Z_P/\kappa_f.
\end{aligned} \tag{A.2}$$

The L-shell ionization matrix elements are evaluated with the help of parametric derivatives of the 1s matrix element (A.2) and are explicitly given in Jakubaßa-Amundsen (1988). With these formulae, the sum over the p states entering into (2.11) is readily evaluated

$$\begin{aligned}
&\sum_{m=0,\pm1}\langle\psi^P_f|\exp(is_z\boldsymbol{e}_z\cdot\boldsymbol{r})|\psi^P_{2p,m}\rangle\langle\psi^P_{2p,m}|\exp[i(\boldsymbol{q}-s_z\boldsymbol{e}_z)\cdot\boldsymbol{r}]|\psi^P_{1s}\rangle\\
&\quad=\frac{3}{2}\frac{Z_P^6N_0}{(p^2+\frac{9}{4}Z_P^2)^3}\frac{A_2^{-i\eta_f-1}(s_z)}{B_2^{2-i\eta_f}(s_z\boldsymbol{e}_z)}\{[(k_f\cos\vartheta_f-v-s_z)M_1(s_z\boldsymbol{e}_z)-s_zM_2(s_z\boldsymbol{e}_z)]\\
&\quad\times(q\cos\vartheta_q-s_z)+k_fq\sin\vartheta_f\sin\vartheta_q\cos(\varphi_q-\varphi_f)M_1(s_z\boldsymbol{e}_z)\}\\
&M_1(\boldsymbol{q}) = (1-i\eta_f)[(2+i\eta_f)+(2-i\eta_f)A_2(q)/B_2(\boldsymbol{q})]\\
&M_2(\boldsymbol{q}) = (1-i\eta_f)i\eta_f+(2+i\eta_f)(1+i\eta_f)B_2(\boldsymbol{q})/A_2(q)
\end{aligned} \tag{A.3}$$

where the relations $\kappa_{fz} = k_f\cos\vartheta_f - v$ and $\boldsymbol{\kappa}_{f\perp} = \boldsymbol{k}_{f\perp}$ have been used, and where $\boldsymbol{p} = \boldsymbol{q} - s_z\boldsymbol{e}_z$. Conveniently, the integration variable φ_q in (2.11) is shifted to $\bar{\varphi}_q = \varphi_q - \varphi_f$.

Appendix 2. Evaluation of the convolution of the Fourier transformed potentials as occur in equations (2.11) and (2.16)

To this aim we introduce the auxiliary integral

$$I_\pm(b,\beta) = \frac{1}{\pi}\int \mathrm{d}\boldsymbol{s}_\perp \frac{1}{s^2+b^2}\frac{1}{(\boldsymbol{s}\pm\boldsymbol{q})^2+\beta^2}. \tag{A.4}$$

Using the abbreviations $\mu = b^2 + s_z^2$ and $\lambda_\pm = \beta^2 + q^2 + s_z^2 \pm 2q_z s_z$, one has, after making the substitution $s_\perp^2 = x$

$$I_\pm(b,\beta) = \frac{1}{\pi}\int_0^\infty s_\perp \,\mathrm{d}s_\perp \int_0^{2\pi} \mathrm{d}\varphi_s \frac{1}{s_\perp^2+\mu}\,\frac{1}{s_\perp^2 \pm 2s_\perp q_\perp \cos\varphi_s + \lambda_\pm}$$

$$= \frac{1}{\sqrt{d}} \ln \frac{\lambda_\pm \sqrt{d} + d + f\mu}{\mu(\sqrt{d}+f)} \tag{A.5}$$

with $d = (\mu - \lambda_\pm)^2 + 4\mu q_\perp^2$ and $f = \lambda_\pm - \mu - 2q_\perp^2$. With the help of this integral, one obtains the result

$$\int \mathrm{d}\boldsymbol{s}_\perp \tilde{V}_\mathrm{T}(\boldsymbol{s})\,\tilde{V}_\mathrm{T}(\boldsymbol{q}-\boldsymbol{s})$$

$$= 2Z_\mathrm{T}^2 \sum_{ij} \left(a_i a_j I_-(b_i, b_j) - 2a_i\alpha_j\beta_j \frac{\mathrm{d}}{\mathrm{d}\lambda_-} I_-(b_i,\beta_j) \right.$$

$$\left. - 2a_j\alpha_i\beta_i \frac{\mathrm{d}}{\mathrm{d}\mu} I_-(\beta_i, b_j) + 4\alpha_i\beta_i\alpha_j\beta_j \frac{\mathrm{d}^2}{\mathrm{d}\mu\,\mathrm{d}\lambda_-} I_-(\beta_i,\beta_j) \right) \tag{A.6}$$

$$\int \mathrm{d}\boldsymbol{s}_\perp \frac{1}{s^2}\,\tilde{V}_\mathrm{T}(\boldsymbol{q}+\boldsymbol{s}) = -(2\pi)^{1/2} Z_\mathrm{T} \sum_i \left(a_i I_+(0, b_i) - 2\alpha_i\beta_i \frac{\mathrm{d}}{\mathrm{d}\lambda_+} I_+(0,\beta_i) \right).$$

Appendix 3. Treatment of the singularities in the elastic contribution (2.11) to ELC

There occur first-order poles in the s_z-integral of (2.11) from the energy denominators at $s_z = s_\mathrm{pol}^{(n)}$ with $s_\mathrm{pol}^{(n)} = (\varepsilon_n - \varepsilon_f)/v$ and $n = 1\mathrm{s}, 2\mathrm{s}, 3\mathrm{s}$ for the degenerate hydrogen-like states. As the remaining integrand $F_n(s_z)$ is well behaved in the vicinity of the pole $s_\mathrm{pol}^{(n)}$, and as all poles are well separated, the integrand can be decomposed into a sum over n, and each contribution treated in the following way

$$\int_{-\infty}^{\infty} \mathrm{d}s_z \frac{1}{vs_z + \Delta E_n + \mathrm{i}\varepsilon} F_n(s_z)$$

$$= \int_{-\infty}^{\infty} \mathrm{d}s_z F_n(s_z) \left[P\frac{1}{vs_z + \Delta E_n} - \mathrm{i}\pi\delta(vs_z + \Delta E_n) \right]$$

$$= \int_{-\infty}^{\infty} \mathrm{d}s_z [F_n(s_z) - F_n(s_\mathrm{pol}^{(n)})] P\frac{1}{vs_z + \Delta E_n}$$

$$+ F_n(s_\mathrm{pol}^{(n)}) \int_{-\infty}^{\infty} \mathrm{d}s_z\, P\frac{1}{vs_z + \Delta E_n} - \frac{\mathrm{i}\pi}{v} F_n(s_\mathrm{pol}^{(n)}) \tag{A.7}$$

where $\Delta E_n = \varepsilon_f - \varepsilon_n$ and P denotes the principal value. The second integral in the above expression vanishes. For a fast convergence it is sufficient to split the integration regime at the three poles, and to make a logarithmic variable substitution in the interval $|s_z| > |s_\mathrm{pol}^{(1\mathrm{s})}|$. In the subsequent integration over q, the lower limit has to be chosen slightly above q_min (e.g. at 1.001 q_min) which does not affect the result, but reduces the required step number in the s_z integration.

References

Atan H, Steckelmacher W and Lucas M W 1990 *J. Phys. B: At. Mol. Opt. Phys.* **23** 2579

Berényi D and Gulyás L 1989 Private communication

Breinig M, Schauer M M, Sellin I A, Elston S B, Vane C R, Thoe R S and Suter M 1981 *J. Phys. B: At. Mol. Phys.* **14** L291

Breinig M, Elston S B, Huldt S, Liljeby L, Vane C R, Berry S D, Glass G A, Schauer M, Sellin I A, Alton G D, Datz S, Overbury S, Laubert L and Suter M 1982 *Phys. Rev.* A **25** 3015

Briggs J S and Drepper F 1978 *J. Phys. B: At. Mol. Phys.* **11** 4033

Briggs J S and Taulbjerg K 1978 *Topics in Current Physics* vol 5 (Berlin: Springer) p 105

Burgdörfer J, Breinig M, Elston S B and Sellin I A 1983 *Phys. Rev.* A **28** 3277

Burgdörfer J 1986 *J. Phys. B: At. Mol. Phys.* **19** 417

Clementi E and Roetti C 1974 *At. Data Nucl. Data Tables* **14** 177

Day M H 1980 *J. Phys. B: At. Mol. Phys.* **13** L65

—— 1981 *J. Phys. B: At. Mol. Phys.* **14** 231

Dettmann K, Harrison K G and Lucas M W 1974 *J. Phys. B: At. Mol. Phys.* **7** 269

Drepper F and Briggs J S 1976 *J. Phys. B: At. Mol. Phys.* **9** 2063

Gayet R 1989 Private communication

Groeneveld K O, Meckbach W and Sellin I A 1984 *Forward Electron Ejection in Ion-Atom Collisions* (Lecture Notes in Physics 213) (Berlin: Springer)

Gulyás L, Szabó Gy, Berényi D, Kövér A, Groeneveld K O, Hofmann D and Burkhard M 1986 *Phys. Rev.* A **34** 2751

Hartley H M and Walters H R J 1987 *J. Phys. B: At. Mol. Phys.* **20** 3811

Holt A R and Moiseiwitsch B L 1968 *J. Phys. B: At. Mol. Phys.* **1** 36

Jakubaßa-Amundsen D H 1981 *J. Phys. B: At. Mol. Phys.* **14** 3139

—— 1988 *Phys. Rev.* A **38** 70

—— 1989a *Int. J. Mod. Phys.* A **4** 769

—— 1989b *Proc. 16th Int. Conf. on Physics of Electronic and Atomic Collisions (New York)* (Amsterdam: North-Holland) Invited Paper

Jensen K E 1986 *Thesis* University of Aarhus

Kim Y-K and Inokuti M 1968 *Phys. Rev.* **165** 39

Knudsen H, Andersen L H and Jensen K E 1986a *J. Phys. B: At. Mol. Phys.* **19** 3341

—— 1986b *Int. Sypo. on Physics of Ionized Gases (Sibenik, Yugoslavia)* Progress Report

Kövér A, Szabó Gy, Berényi D, Gulyás L, Cserny I, Groeneveld K O, Hofmann D, Koschar P and Burkhard M 1986 *J. Phys. B: At. Mol. Phys.* **19** 1187

Lucas M W and Steckelmacher W 1987 *Lecture Notes in Physics* vol 294 (Berlin: Springer) p 229

Man K F, Steckelmacher W and Lucas M W 1986a *J. Phys. B: At. Mol. Phys.* **19** 401

—— 1986b *J. Phys. B: At. Mol. Phys.* **19** 4171

McDowell M R C and Coleman J P 1970 *Introduction to the Theory of Ion-Atom Collisions* (Amsterdam: North-Holland) p 364

Meckbach W, Nemirovsky I B and Garibotti C R 1981 *Phys. Rev.* A **24** 1793

Oswald W, Schramm R and Betz H-D 1989 *Phys. Rev. Lett.* **62** 1114

Rule D W 1977 *Phys. Rev.* A **16** 19

Shakeshaft R and Spruch L 1978 *Phys. Rev. Lett.* **41** 1037

Strand T G and Bonham R A 1964 *J. Chem. Phys.* **40** 1686